Band-gap transition induced by interlayer van der Waals interaction in MoS_2

S. W. Han,[1] Hyuksang Kwon,[2] Seong Keun Kim,[2] Sunmin Ryu,[3] Won Seok Yun,[1] D. H. Kim,[4] J. H. Hwang,[4] J.-S. Kang,[4] J. Baik,[5] H. J. Shin,[5] and S. C. Hong[1,*]

[1]*Department of Physics and Energy Harvest-Storage Research Center, University of Ulsan, Ulsan 680-749, Korea*

[2]*Deparment of Chemistry and Department of Biophysics and Chemical Biology, Seoul National University, Seoul 151-747, Korea*

[3]*Department of Applied Chemistry, Kyung Hee University, Yongin, Gyeonggi 446-701, Korea*

[4]*Department of Physics, The Catholic University of Korea, Bucheon 420-743, Korea*

[5]*Pohang Accelerator Laboratory (PAL), POSTECH, Pohang 790-784, Korea*

(Received 12 April 2011; revised manuscript received 16 May 2011; published 6 July 2011)

We have investigated the electronic structures of single- and double-layered MoS_2, composing of heterojunction structures such as graphene, MoS_2, and SiO_2 and MoS_2 and SiO_2, using scanning photoelectron microscopy. Negative shifts of both core levels and valence bands toward the Fermi energy have been observed. In connection with first-principles calculations, we have confirmed that the direct gap of single-layer MoS_2 is changed to an indirect gap by stacking additional layers via van der Waals interlayer interactions.

DOI: 10.1103/PhysRevB.84.045409 PACS number(s): 73.20.At, 73.22.−f, 73.30.+y, 79.60.−i

I. INTRODUCTION

Recently, thickness-dependent modulation of the optical band-gap (E_G)[1] and phonon frequency[2] has been observed when the molybdenum disulfide (MoS_2) thickness was decreased to a single-layer (S-Mo-S) obtained by employing the microexfoliation technique.[3] The crystal structure of MoS_2 consists of a Mo atom layer sandwiched between two sulfur layers in a trigonal prismatic arrangement[4] [see bottom of Fig. 5(b)]. The Mo-S bonds are strongly covalent, but the sandwich layers are coupled only by weak van der Waals (vdW) interactions, resulting in easy slippage as well as easy cleavage of planes. The optical E_G of bulk MoS_2, in which indirect (∼1.3 eV) and direct (∼1.9 eV) gaps coexist, expands to an indirect gap of ∼1.6 eV in double-layer MoS_2 and then to a direct gap of ∼1.9 eV in single-layer MoS_2.[5] In other words, the direct gap of single-layer MoS_2 can be changed to an indirect gap by stacking additional layers by vdW interlayer interactions. It has been suggested that the electronic properties of MoS_2 have a strong dependence on the number and distance of planes composing the system.[6] On the other hand, MoS_2 nanosolid deposited on Au (111) appeared to have metallic states for sizes smaller than 3 nm due to quantum confinement effects.[7,8] The origin of the thickness-induced changes in the E_G of MoS_2 is yet unclear.

In combination with the previous results of optical spectroscopy for unoccupied states,[1,5] the electronic structures of the graphene and MoS_2 heterojuction,[9,10] including pristine MoS_2 samples of very few layers, have been investigated using scanning photoelectron microscopy (SPEM) to determine the occupied states.[11,12] The graphene overlayer[10] circumvents the charging effects that can perturb the observed spectra on pristine MoS_2 layers. Photoemission spectroscopy (PES) is a sensitive probe for studying the electronic structure of a solid at a surface that may be different from its bulk counterpart due to atomic coordination imperfections and different atomic geometries at the surface.[13] The line shapes of the core-level PES spectra and their energy positions are sensitive to the local chemical state and the electronic structures, and so PES can provide direct insight into the nature of the interface bond. In particular, SPEM is a powerful tool for obtaining chemical information at the local area of the surface.[11,12]

II. EXPERIMENTAL AND COMPUTATIONAL PROCEDURE

Single- and few-layer MoS_2 films were deposited onto Si substrates with a 285-nm-thick SiO_2 layer by exfoliating bulk crystals of 2H-MoS_2 (SPI, natural molybdenite) according to the micromechanical exfoliation method.[3] The thickness of the films was characterized by employing micro-Raman spectroscopy,[2] which was operated with an Ar ion laser at 514.5 nm. The excitation laser beam of an average power less than 2.5 mW was focused onto samples of interest by a 40× objective lens (NA = 0.60). Backscattered light consisting of Raman and photoluminescence (PL) signals was collected by the objective. There was no detectable change caused by laser irradiation throughout the measurements. Composite structures of graphene, MoS_2, and SiO_2 were prepared by transferring chemical vapor deposition (CVD)-grown graphene onto the MoS_2 and SiO_2 samples.[14] The thickness and structural quality of the graphene overlayer were characterized by Raman spectroscopy as well.[15]

SPEM measurements were performed at the 8A1 undulator beamline of the Pohang Accelerator Laboratory (PAL) at room temperature under a base pressure better than 3×10^{-10} Torr. SPEM images were obtained by using the selected energy channels, i.e., Si 2*p* (96–108 eV), S 2*p* (156–168 eV), and Mo 3*d* (227–239 eV) photoelectrons, to identify the location and geometry of samples. After taking the SPEM images, microspot PES spectra of core levels and valence-bands were obtained by locating the focused beam to the specific locations. The lateral resolution in the SPEM mode was approximately 0.5 μm at a photon energy of 620 eV. The spectral energy resolution was about 500 meV, which was determined from the valence spectrum of Au films in the normal mode. By comparing the core-level PES spectra obtained in the SPEM mode with those obtained in the normal mode, it was confirmed that there are no significant differences in the energy resolutions of the SPEM and normal modes.

To resolve how the electronic structure of MoS_2 has been influenced by the number of planes through the vdW interlayer interaction, first-principle calculations were performed using the full-potential linearized augmented plane wave (FLAPW) method.[16] The general gradient approximation (GGA)[17] was

adopted to describe the exchange-correlation potential. Energy cutoffs of 12.25 Ry and 256 Ry were employed for the basis expansion and the charge-potential within the interstitial region, respectively. We used experimental values (a = 3.160 Å, c = 12.294 Å)[4] for the bulk calculation as well as fully optimized atomic structures. In the film calculation using single-slab geometry, the two-dimensional lattice constant was fixed at a = 3.160 Å, and the vertical positions of all atoms were optimized according to atomic forces. Convergence with respect to the number of K-points was carefully checked.

III. RESULTS AND DISCUSSION

Due to the optical interference effects,[18] graphene and MoS_2 single layers in a composite sample are clearly visible in the optical micrograph, as shown in Fig. 1(a). Single (1L) and double layers (2L) of MoS_2 gave a larger optical contrast than graphene and could still be identified after the deposition of a graphene overlayer. Some fraction of the sample surfaces was not covered by a graphene overlayer due to the incomplete transfer of graphene, which is denoted as "SiO_2" in Fig. 1(a).

In 1L and 2L MoS_2 films, two prominent Raman bands, in-plane E^1_{2g} and out-of-plane A_{1g} modes, show systematic frequency progressions as a function of thickness.[2] In particular, it was shown that the frequency difference between the two bands serves as a precise indicator of the film thickness.[2] Frequency differences in 1L and 2L MoS_2, shown in Fig. 1(b), are consistent with the values in the literature[2] within $\pm 0.5\ cm^{-1}$. The graphene overlayer can be identified by the characteristic G and 2D bands and lack of a disorder-related D band, which indicates the high structural quality of the films in this work [see Fig. 1(b)].[15] The broad spectral features located at >1600 cm^{-1}, denoted as PL in Fig. 1(b), are due to the photoluminescence (PL) from 1L MoS_2 or 2L MoS_2.[1] The coexistence of Raman and PL bands from graphene and MoS_2 confirms that the composite structures have been successfully formed in the films employed in this work.

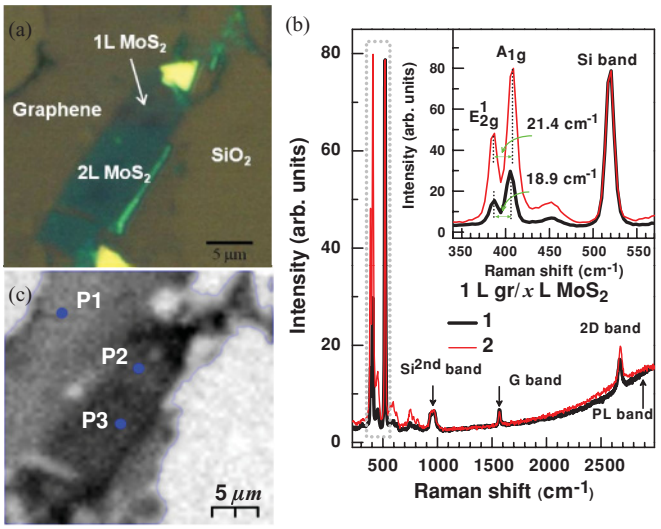

FIG. 1. (Color online) (a) Optical image of 1L and 2L MoS_2 on SiO_2 substrate, covered by 1L graphene. Yellow flakes are multilayered MoS_2. (b) Raman spectra for 1L graphene and 1L (black) or 2L (red) MoS_2. Both G and 2D bands originate from the graphene, while Si^{2nd} and PL bands come from the underlying Si substrate and MoS_2, respectively. The magnified inset shows detailed Raman spectra in the dotted box. The frequency difference between two Raman bands of MoS_2 (E^1_{2g} and A_{1g}) is 18.9 cm^{-1} and 21.4 cm^{-1} for 1L and 2L MoS_2, respectively. All spectra were normalized by the Si Raman band at 520 cm^{-1}.(c) 30 × 30 μm^2 SPEM image of the 1L and 2L MoS_2 on the SiO_2 substrate, covered by 1L graphene (dark regions). Spot P1 indicates graphene directly deposited onto the SiO_2 substrate. 1L MoS_2 is denoted as P2 and 2L MoS_2 is denoted as P3. Bright regions correspond to the bare SiO_2 substrate.

Figure 2(a) shows the carbon (C) 1s core-level PES spectra (open circles) and the curve-fitting results, including the total sum (black lines) and the components (colored lines) in the binding energy (BE) scale. These C 1s spectra were obtained at different spots, marked P1, P2, and P3 in the 30 × 30 μm^2 SPEM image [see Fig. 1(c)]. The SPEM image was obtained by selecting the S 2p (156–168 eV) energy channel. The photoelectrons from graphene and SiO_2 also have strong background photoelectrons in this energy range and result in the rather reverse contrast distribution. The image is similar to the optical microscope image and shows the microstructures of 1L MoS_2 (spot P2) and 2L MoS_2 (spot P3), both of which are covered with graphene (dark regions). Spot P1 indicates graphene directly deposited onto the SiO_2 substrate without MoS_2 films. Bright regions correspond to the bare SiO_2 substrate.

The measured C 1s PES spectra (Fig. 2) show the different line shapes and intensity distributions. For comparison, all the spectra were scaled to have the same. Line shapes from different regions provide clear evidence for the thickness dependence of MoS_2 layers. In Fig. 2, we show the C 1s spectrum of highly oriented pyrolytic graphite (HOPG) as a reference spectrum, which was obtained in the normal mode; PES spectra were obtained without focusing the incident

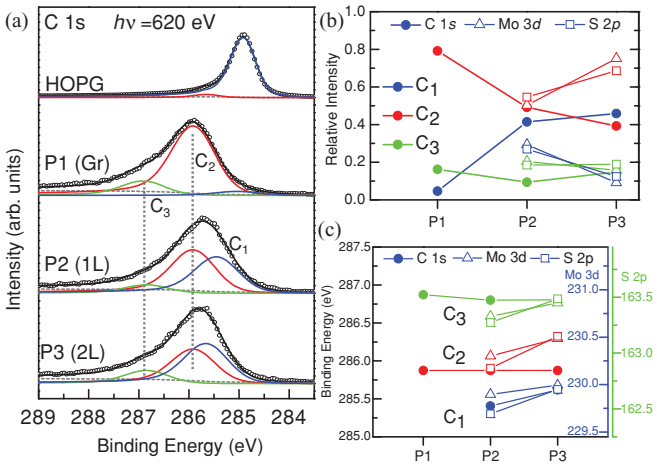

FIG. 2. (Color online) (a) C 1s core-level PES spectra (open circles), obtained at the spots marked as P1, P2, and P3 in the SPEM image, shown in Fig. 1(c), along with the curve-fitting results (lines). (b) Plot of the relative intensity for the three components, C_1 (blue), C_2 (red), and C_3 (green), of C 1s (solid circles), Mo 3d (open triangles), and S 2p (open squares) core-level spectra, normalized to the total intensity as a function of the thickness of MoS_2 layer. (c) The variation of the binding energy of the components.

x-rays. The C 1*s* spectrum of HOPG shows a narrow peak at 284.90 eV and has an asymmetric line shape on the higher BE side, indicating the presence of sp^2 hybridized C–C bonds.[19] On the other hand, the C 1*s* peak, obtained from the graphene and SiO_2 (P1), is broader and located at a higher BE than that of HOPG. This is probably due to the poor electrical conductivity of the SiO_2 substrate relative to HOPG and is in accordance with a previous report related to graphene on a SiO_2 substrate.[20]

In order to obtain microscopic information from the core-level spectra, we decomposed the C 1*s* PES spectra into different components to separate out surface and interface reaction products. Deconvolution fits were performed by means of Doniach-Šunjić functions.[21] For each component, the natural (Lorentzian) line width, representing the core-hole lifetime, was determined to be ~0.13 eV, and the asymmetry parameter (or singularity index, α), reflecting the density of states at the Fermi energy, E_F, was determined to be ~0.09 while the Gaussian width was fixed at the instrumental resolution of 0.50 eV.

Based on previous angle-resolved core-level PES studies of graphite,[19] the spectrum of HOPG was fitted with two components. The high-energy (low-kinetic energy) component (285.60 eV, red solid line) represents the surface contribution due to surface interlayer contraction, while the low-energy (high-kinetic energy) component (284. 90 eV, blue solid line) represents the bulk origin. By employing these parameters, the other spectra (P1–P3) were also fitted. In fitting these other spectra, however, a larger Gaussian width of ~0.92 eV was needed. In addition, a third component (C_1, blue solid lines) was required to fit these spectra, while only two components were enough for fitting HOPG. We believe that, in the case of the graphene-overlayer on 1L MoS_2 (P2) and 2L MoS_2 (P3), this third component (C_1, blue lines) originates from the interaction of graphene with MoS_2 layers. As to graphene (P1), the negligible intensity of the third component is possibly attributed to the weak interaction of graphene with the SiO_2 substrate.[20,22]

For clarity, as shown in Fig. 2(b), the relative intensity of component C_1 (blue circles with lines), relating to the contribution from the MoS_2 layers, increases with increasing thickness of the MoS_2 layer while that of component C_2 (red circles with lines), relating to the contribution from the graphene overlayer, decreases. On spots P2 and P3, the intensities of two components, C_1 and C_2, are comparable due to the constant probing depth at a fixed photon energy of 620 eV, in which the corresponding attenuation length (λ) of C 1*s* photoelectrons is approximately 8 Å.[22] The intensity of the other component C_3, (green circles with lines), probably relating to the contribution from contamination on the surface, is almost constant.

In addition, as shown in Fig. 2(c), component (C_1) is found to shift by ~0.20 eV toward E_F from ~285.6 eV (P3) to ~285.4 eV (P2), while the other components (C_2 and C_3, vertical dots) were fixed at ~285.9 eV and 286.8 eV, respectively. It is notable that the reduction in MoS_2 thickness results in a shift toward E_F, i.e., a negative shift. Considering the positive shift in the C 1*s* core level of graphene compared to that of HOPG, the negative shift clearly excludes the charging effect due to poor screening of the core hole.

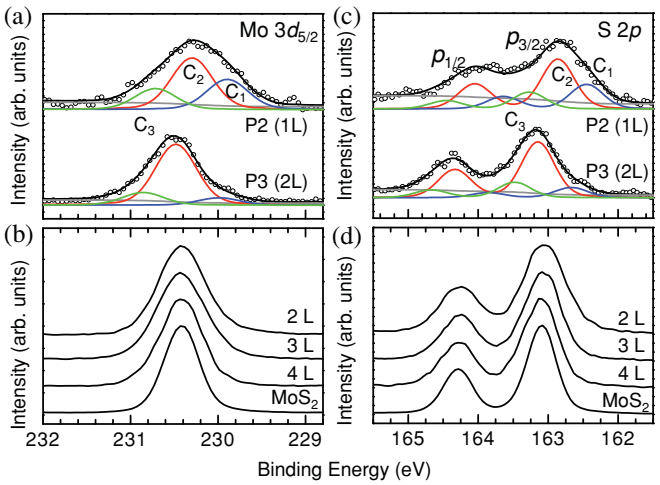

FIG. 3. (Color online) (a–b) Photoemission spectra of Mo 3$d_{5/2}$ core levels, obtained at $h\nu = 620$ eV, along with the curve-fitting results. (c–d) Similarly for S 2*p* core levels. The spectra in (a) and (c) were obtained from the graphene overlayer on 1L MoS2 (P2) and 2L MoS2 (P3), respectively, while those in (b) and (d) were obtained from pristine few-layer MoS_2 and bulk MoS_2, respectively.

Concurrent negative shifts of both Mo 3*d* and S 2*p* peaks were also observed, as shown in Figs. 3(a) and 3(c). Upon lowering the thickness, from 2L (P3) to 1L (P2), both Mo 3*d* and S 2*p* core-level line spectra became much broader. Unlike the case of C 1*s*, for the deconvolution of Mo 3*d* and S 2*p*, the Lorentzian width and asymmetry parameter were fixed at 0.1 eV and 0, respectively, as was used in the literature,[23] while maintaining the same Gaussian width of 0.5 eV. The values of the spin-orbit splitting ($\Delta E_S O$) and the branching ratios [$I(3d_{5/2})/I(3d_{3/2})$ and $I(2p_{3/2})/I(2p_{1/2})$] were 3.10 eV and 0.67 for Mo 3*d* peaks and 1.19 eV and 0.5 for S 2*p* peaks, respectively.

With decreasing thickness of the MoS_2 layer from 2L (P3) to 1L (P2), the relative intensity of component C_1 (blue solid lines) increased, but that of component C_2 (red solid lines) decreased, while component C_3 (green solid lines) remains largely unchanged. As summarized in Fig. 2(b), the variation in relative intensity between C_1 and C_2 of both Mo 3*d* and S 2*p* spectra is opposite that of C 1*s* spectra. Hence, the three components of both Mo 3*d* and S 2*p* spectra, from high to low BE, can be assigned to the contribution of the interaction of the MoS_2 layer with the graphene layer, the MoS_2 layer and the SiO_2 substrate, respectively. This definition is reasonable based on the analysis of C 1*s* spectra, where the surface component appears at a higher BE than the bulk.

On the other hand, as the thickness of MoS_2 layers decrease, all peaks clearly shifted toward a lower BE by ~0.2 eV for Mo 3*d* and by ~0.3 eV for S 2*p*, which is consistent with the trend in the C 1*s* spectra (see Fig. 2(c)). These shifts in the core-level PES spectra are quite similar to the expansion of E_G from 1.6 eV in the double layer to 1.9 eV in the single layer, which was obtained via optical spectroscopy.[1,5] Although the charging effect of the SiO_2 substrate, which induces a positive shift of the core levels, could be excluded, one can surmise that the core-level shift toward a lower BE is due to the influence of the graphene overlayer. In addition, we need to consider

the significant influence of the underlying SiO_2 substrates in the single layer of MoS_2, because it has been found that the interaction of the substrate has a negligible effect on the novel properties of MoS_2.

For this reason, pristine samples with only a few layers of MoS_2 were prepared. Figures 3(b) and 3(d) also show the Mo 3*d* and S 2*p* spectra obtained using SPEM. Unfortunately, we could not avoid charging effects on these samples due to the bad screening capabilities. The peak of each spectrum was aligned to that of bulk MoS_2, which was obtained in the normal mode and had a negligible charging effect. Upon lowering the thickness, the full width at half maximum (FWHM) of both Mo 3*d* and S 2*p* spectra increases from ∼0.5 eV to ∼0.7 eV. This broadening seems to reflect the negative shifts of core levels since the natural lifetime widths are not expected to vary much.

Figure 4 compares the valence-band PES spectra of the MoS_2 layers covered with graphene (P2, P3) to those of the pristine MoS_2 layers. The bottom of Fig. 4 (P1) shows the graphene bands, obtained from graphene directly deposited onto the SiO_2 substrate, where the broad feature at ∼8.5 eV corresponds to the π bands. Upon increasing the thickness of the MoS_2 layer (from P2 to P3), the bands related to the MoS_2 become clearly visible, and their intensities increase, while the intensity of the graphene bands are suppressed.

For the case of the pristine MoS_2 layers, the binding energies were also corrected by aligning the S 3*s* peak of each spectrum, located at ∼15 eV, to that of bulk. There are several distinct features in the BE region, up to 9 eV below E_F. These are associated with the *d* orbitals of Mo atoms and *p*-orbitals of S atoms, which result from the bonding and nonbonding interactions.[4] The intensity close to E_F is negligible, consistent with the semiconducting nature of MoS_2. The valence-band maxima (VBM) of MoS_2 are located ∼2 eV below E_F [see also Fig. 4(b)]. Although the data are rather noisy, a negative shift toward E_F is observed in 1L MoS_2 (P2) as indicated with an arrow and is more evident in the enlarged figure, shown in Fig. 4(b), even though the amount of the shift is small. This shift agrees well with the behavior of core-level PES spectra. However, these negative shifts toward E_F, which imply a rigid-band shift without a band-gap expansion, seem to contradict the band-gap expansion due to the band-gap transition observed in the optical spectroscopies.[1,5]

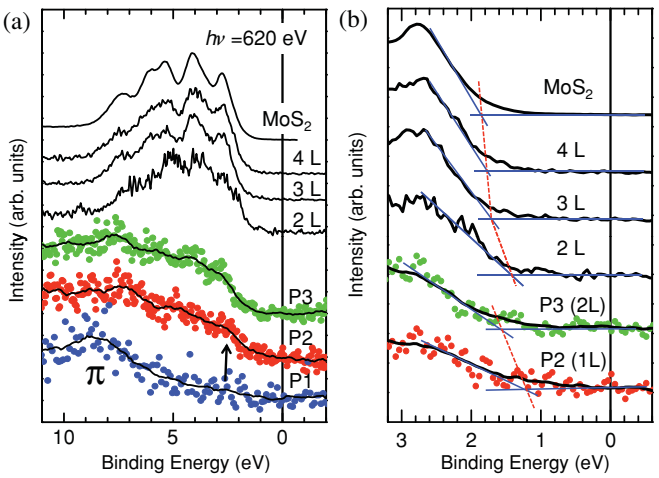

FIG. 4. (Color online) (a) Valence-band PES spectra obtained at $h\nu = 620$ eV. The spectra of P1–P3, with smoothed lines (black solid lines) for clarity, were obtained from the graphene overlayer sample. Others were obtained from pristine few-layer and bulk MoS_2. (b) Near the Fermi energy, enlarged from (a).

In order to elucidate the experimentally observed negative shifts, we calculated the thickness dependence of band structures for (a) bulk MoS_2, (b) 2L, and (c) 1L MoS_2 by using the FLAPW method as shown in Fig. 5 The overall feature of the present calculated band structures is quite consistent with the previous pseudopotential ones.[1,6] The indirect gap of the bulk is ∼0.9 eV and consists of the VBM (horizontal solid lines), which are set to zero in order to clarify the band gap, at the Γ-point and the conduction-band minima (CBM, horizontal dotted lines) at the center between Γ- and *K*-points, indicated by open circles. This indirect gap increases to ∼1.3 eV in the 2L MoS_2. Interestingly, the position of the CBM has been changed to a *K*-point with a smaller energy difference from that of the center point, which has been determined in the previous results.[1,6] Then, in the 1L MoS_2, the band gap becomes the direct gap of ∼1.7 eV between the VBM and CBM at the *K*-point as no noticeable vdW interlayer interaction is present. This is consistent with thickness-induced characteristics observed by Raman spectroscopy that the E^1_{2g} (in-plane) vibration frequency increases, while the A_{1g} (out-plane) vibration frequency decreases with decreasing sample thickness.[2] In addition, an angle-resolved PES (ARPES)[24] experiment on an isoelectronic compound WS_2 also showed that while the VBM of bulk was located at the Γ-point, that of a single layer was determined at the *K*-point, which was in agreement with the theoretical calculation.[25] Furthermore, theoretical calculations on WSe_2 showed the same trend.[26]

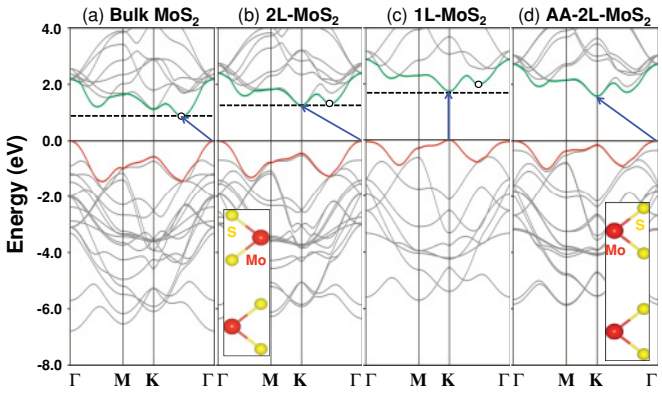

FIG. 5. (Color online) The horizontal solid lines in each panel indicate the VBM being set to zero in order to clarify the band gap. The horizontal dotted lines indicate the CBM. The solid arrows indicate the lowest energy transitions. (a) Bulk MoS_2 is characterized by an indirect band gap. (b) 2L MoS_2 remains the indirect band gap, but the CBM is located at *K*-point. The bottom shows the unit cell of side view for the *AB* stacking. (c) 1L MoS_2 becomes a direct band-gap semiconductor. (d) Indirect band gap of *AA*-2L MoS_2 is larger than that of (b) due to the geometry-induced effects of the vdW interaction. The bottom shows the unit cell of side view for the *AA* stacking.

Looking in detail, the valence bands at the *K*- and the Γ-points originate mostly from the $d_{xy/x2-y2}$ and the $d_z{}^2$ of the Mo atoms, respectively, whereas the conduction band at the *K*-point consists of mainly the $d_z{}^2$ of the Mo atoms and the band near the center point between Γ- and *K*-points consists of mixed orbitals between the $d_{xy/x2-y2}$ and $d_z{}^2$ of the Mo atoms. Considering the experimentally observed negative-shifts toward E_F, it seems that the valence band has a strongly thickness dependence in the *K*-point. In fact, however, it is difficult due to uncertainty in the determination of the Fermi level. When the vacuum level is taken as a reference, the state at the Γ-point may shift depending on the thickness, as the claim of the previous studies.[1,6] For clarity, this argument should be studied in the future by employing more direct and detailed methods such as ARPES.

On the other hand, to see the geometry-induced effects of the vdW interaction, we investigated AA-2L MoS_2 (*AA* stacking) where the Mo atoms of the upper sandwich layer (single layer) are just above the Mo atoms of the lower sandwich layer as shown in Fig. 5(d). In the structure of bulk 2H-MoS_2 or 2L MoS_2, the Mo atoms of the upper sandwich layer are directly above the S atoms of the lower sandwich layer (*AB* stacking).[4] The interlayer distance of AA-2L MoS_2 increases to 3.85 Å from the 3.07 Å of 2L MoS_2 based on atomic force calculations, but the indirect gap remains unchanged despite the enhancement in E_G (∼1.6 eV). Our results clearly demonstrate that the weak vdW interlayer interaction alters the band structure of MoS_2 crystals. In addition, considering no significant difference exists in the band structures between the vdW-bonded graphite[27] and graphene, the reason why the band structure of MoS_2 crystals has a strong thickness-dependence could be the *d* orbitals of Mo atoms.

IV. SUMMARY

In the single- and double-layered MoS_2, we have observed the thickness-dependent negative shifts of both core levels and valence bands toward the Fermi energy using SPEM. We have revealed that the direct gap of single-layer MoS_2 is changed to an indirect gap by vdW interlayer interactions. This fact indicates that the design of hybrid structures using the single layers for applications from electronics to energy storage requires a new route instead of adjacent sheets stacked via vdW interactions such as a hafnium oxide, HfO_2, which has been found to enhance the mobility of single-layer MoS_2.[28]

ACKNOWLEDGMENTS

The authors are grateful to Byung Hee Hong for his generous donation of the CVD-grown graphene. This work was supported by Priority Research Centers Programs (Grant No. 2009-0093818) and Basic Research Programs (Grant No. 2010-0008842). Work at the CUK was supported by the National Research Foundation (NRF) of Korea under Contract No. 2009-0064246. This research was also supported by the Basic Science Research Program (Grant No. 2010-0015363, S.R.) through the NRF funded by the Ministry of Education, Science, and Technology (MEST). The experiment at PAL was supported by POSTECH and MEST in Korea.

*schong@ulsan.ac.kr

[1] A. Splendiani, L. Sun,Y. Zhang, T. Li, J. Kim, C.-Y. Chim, G. Galli, and F. Wang, Nano Lett. **10**, 1271 (2010).

[2] C. Lee, H. Yan, L. E. Brus, T. Heinz, J. Hone, and S. Ryu, ACS Nano **4**, 2695 (2010).

[3] K. S. Novoselov, D. Jiang, F. Schedin, T. Booth, V. V. Khotkevich, S. V. Morozov, and A. K. Geim, Proc. Natl. Acad. Sci. USA **102**, 10451 (2005).

[4] Th. Böer, R. Severin, A. Müller, C. Janowitz, R. Manzke, D. Voss, P. Krüger, A. Mazur, and J. Pollmann, Phys. Rev. B **64**, 235305 (2001).

[5] K. F. Mak, C. Lee, J. Hone, J. Shan, and T. F. Heinz, Phys. Rev. Lett. **105**, 136805 (2010).

[6] T. S. Li and G. L. Galli, J. Phys. Chem. C **111**, 16192 (2007).

[7] S. Helveg, J. V. Lauritsen, E. Laegsgaard, I. Stensgaard, J. K. Nørskov, B. S. Clausen, H. Topsøe, F. Besenbacher, Phys. Rev. Lett. **84**, 951 (2000).

[8] M. V. Bollinger, J. V. Lauritsen, K. W. Jacobsen, J. K. Nørskov, S. Helveg, and F. Besenbacher, Phys. Rev. Lett. **87**, 196803 (2001).

[9] J. Kibsgaard, J. V. Lauritsen, E. Lægsgaard, B. S. Clausen, H. Topsøe, and F. Besenbacher, J. Am. Chem. Soc. **128**, 13950 (2006).

[10] By using the Vienna *ab initio* simulation package (VASP) code, it has been revealed that the interlayer distance between the graphene and single layer of MoS_2 is approximately 3.85 Å, and the graphene overlayer has a negligible effect on the novel properties of MoS_2.

[11] M. K. Lee and H. J. Shin, Rev. Sci. Instrum. **72**, 2605 (2001).

[12] J.-S. Kang, G. Kim, S. C. Wi, S. S. Lee, S. Choi, S. Cho, S. W. Han, K. H. Kim, H. J. Song, H. J. Shin, A. Sekiyama, S. Kasai, S. Suga, and B. I. Min, Phys. Rev. Lett. **94**, 147202 (2005).

[13] C. Q. Sun, Phys. Rev. B **69,** 045105 (2004).

[14] S. K. Bae, H. Kim, Y. Lee, X. Xu, J.-S. Park, Y. Zheng, J. Balakrishnan, T. Lei, H. R. Kim, Y. I. Song, Y.-J. Kim, K. S. Kim, B. Øzyilmaz, J.-H. Ahn, B. H. Hong, and S. Iijima, Nature. Nanotech. **5**, 574 (2010).

[15] A. C. Ferrari, J. C. Meyer, V. Scardaci, C. Casiraghi, M. Lazzeri, F. Mauri, S. Piscanec, D. Jiang, K. S. Novoselov, S. Roth, and A. K. Geim, Phys. Rev. Lett. **97**, 187401 (2006).

[16] E. Wimmer, H. Krakauer, M. Weinert, and A. J. Freeman, Phys. Rev. B **24**, 864 (1981); M. Weinert, E. Wimmer, and A. J. Freeman, *ibid.* **26**, 4571 (1982).

[17] J. P. Perdew, K. Burke, and M. Ernzerhof, Phys. Rev. Lett. **77**, 3865 (1996).

[18] S. Roddaro, P. Pingu, V. Piazza, V. Pellegrini, and F. Beltram, Nano Lett. **7**, 2707 (2007).

[19] M. R. C. Hunt, Phys. Rev. B **78**, 153408 (2008).

[20] K.-J. Kim, H. Lee, J.-H. Choi, Y.-S. Youn, J. Choi, H. Lee, T.-H. Kang, M. C. Jung, H. J. Shin, H.-J. Lee, S. Kim, and B. Kim, Adv. Mater. **20**, 3589 (2008).

[21] S. Doniach and M. Súnjic, J. Phys. C **3**, 285 (1970).

[22] Z. Q. Luo, T. Yu, K.-J. Kim, Z. Ni, Y. You, S. Lim, Z. Shen, S. Wang, and J. Lin, ACS Nano **3**, 1781 (2009).

[23] S. Mattila, J. A. Leiro, M. Heinonen, and T. Laiho, Surf. Sci. **600**, 1168 (2006).

[24] A. Klein, S. Tiefenbacher, V. Eyert, C. Pettenkofer, and W. Jaegermann, Phys. Rev. B **64**, 205416 (2001).

[25] K. Albe and A. Klein, Phys. Rev. B **66**, 073413 (2002).

[26] D. Voss, P. Krüger, A. Mazur, and J. Pollmann, Phys. Rev. B **60**, 14311 (1999).

[27] J. D. Lee, S. W. Han and J. Inoue, Phys. Rev. Lett. **100**, 216801 (2008).

[28] B. Radisavljevic, A. Radenovic, J. Brivio, V. Giacometti, and A. Kis, Nature Nanotechnol. **6**, 147 (2011).